Talanta 106 (2013) 192–199

Contents lists available at SciVerse ScienceDirect

Talanta

journal homepage: www.elsevier.com/locate/talanta

Direct electrochemistry of cholesterol oxidase immobilized on gold nanoparticles-decorated multiwalled carbon nanotubes and cholesterol sensing

Lian Zhu [a], Lili Xu [a], Liang Tan [a,*], Hao Tan [b], Sufang Yang [a], Shouzhuo Yao [a]

[a] Key Laboratory of Chemical Biology and Traditional Chinese Medicine Research (Ministry of Education of China), College of Chemistry and Chemical Engineering, Hunan Normal University, Changsha 410081, China
[b] The Maternal and Child Health Hospital of Hunan Province, Changsha 410008, China

ARTICLE INFO

Article history:
Received 12 October 2012
Received in revised form
20 December 2012
Accepted 21 December 2012
Available online 31 December 2012

Keywords:
Nanocomposite
Cholesterol oxidase
Direct electrochemistry
Cholesterol biosensor

ABSTRACT

An electrochemical cholesterol biosensor based on the direct electron transfer of cholesterol oxidase (ChOx) immobilized on gold nanoparticles-decorated multiwalled carbon nanotubes (GNPs-MWCNTs) was fabricated. GNPs-MWCNTs were prepared based on the reduction of $HAuCl_4$ in the presence of carboxyl group functionalized MWCNTs. Transmission electron microscopy image shows that rounded gold nanoparticles with diameters of 6–10 nm were decorated on carbon nanotube surfaces. ChOx was directly adsorbed on the nanocomposite modified glassy carbon electrode and protected by a Nafion film. Direct electrochemistry of ChOx on the electrode surface was obtained, proved by one pair of well-defined, quasi-reversible redox peaks in phosphate buffered saline. Under optimized conditions, the fabricated electrode displayed a linear response in the cholesterol concentration range from 0.0100 to 5.00 mmol L^{-1} with a detection limit of 4.3 μmol L^{-1} estimated at a signal-to-noise ratio of 3. The apparent Michaelis–Menten constant was measured to be 0.29 mmol L^{-1}, indicating that the immobilized ChOx on GNPs-MWCNTs matrix retained its native activity. The developed biosensor presented good selectivity, repeatability, reproducibility and stability. The concentration of free cholesterol in a human serum sample, detected by using the developed biosensor, is in good agreement with that determined by the well-established spectrophotometric method.

1. Introduction

Cholesterol is a ubiquitous component in cells and tissues of animals, either participating the construction of cell membranes or serving as a biosynthetic precursor of bile acids, vitamin D, steroid hormones (glucocorticoids, estrogens, progesterones, androgens and aldosterone) and so on [1]. It is produced by liver and circulates in blood, playing an important role in the brain, nervous and immune systems of humans. A diet high in saturated fats and cholesterol can raise blood cholesterol levels. Excess cholesterol that is not taken up by body cells may be deposited in the walls of arteries, resulting in some deadly diseases including arteriosclerosis, cerebral thrombosis, myocardial infarction and lipid metabolic disturbance [2]. Therefore, cholesterol is one of the most frequently determined analytes in clinical as well as in analysis of food samples. Developing rapid, sensitive and simple detection methods for cholesterol has great significance in practical applications.

Non-enzymatic techniques including spectrophotometric [3] gas–liquid chromatography [4] and HPLC [5] methods have been reported for the analysis of cholesterol in food and clinical samples. Some methods, such as spectrophotometry based on the Liebermann–Burchard reaction [3], usually involve complex procedure for the precipitation of lipoprotein fractions and present certain disadvantages, such as lack of specificity and selectivity because of the interfering reactions and use of unstable and corrosive reagents. Due to the simplicity, rapidness and cost, enzymatic procedures have gradually replaced the chemical methods based on the classical Libermann–Burchard reaction. The electrochemical methods based on cholesterol oxidase (ChOx) are extremely attractive for the determination of cholesterol because of its advantages in inexpensiveness and also its freedom from pre-separation procedures. Among these, some biosensors are based on the detection of electrooxidation of hydrogen peroxide produced during the catalytic oxidation reaction of cholesterol in the presence of ChOx [6–8]. It requires a high anodic potential [9] that may induce simultaneous oxidation

* Corresponding author. Tel./fax: +86 731 8882 2046.
E-mail address: liangtan@hunnu.edu.cn (L. Tan).

0039-9140/$ - see front matter © 2012 Elsevier B.V. All rights reserved.
http://dx.doi.org/10.1016/j.talanta.2012.12.036

of other electroactive species in samples, such as ascorbic acid and uric acid, and lead to false positive signals. Therefore, the second-generation enzyme biosensor using electron mediator is employed. A reduced mediator is formed instead of hydrogen peroxide and then reoxidized at the electrode, providing an amperometric signal [10,11]. In recent years, some cholesterol electrochemical biosensor researches focused on the direct electron transfer between ChOx and electrode surfaces [12–14]. However, some problems, including the poor compatibility of the support matrix and the deep embedment of redox active site in the protein, may restrict the analytical efficiency of the developed biosensor. Developing suitable support matrix that either provides better environment for the efficient enzyme loading or maintain the enzymatic bioactivity is one of critical factors.

Carbon nanotubes (CNTs) have been recognized as one of the most promising electrode materials due to their high chemical stability, good electrical conductivity, and tubular structure [15]. CNTs-based modified electrode exhibits excellent electron transfer capabilities for the oxidation of biomolecules such as cytochrome c [16], NADH [17], dopamine, ascorbic acid and uric acid [18]. This material can provide high surface area and compatible microenvironment for enzyme loading to retain its bioactivity. The similarity in length scales between nanotubes and redox enzymes suggests interactions that may be favorable for biosensor electrode applications. The immobilization of glucose oxidase [19,20], horseradish peroxidase [21,22], cholesterol oxidase [12,13] on CNTs and their analytical application have been reported. It is well known that gold nanoparticles (GNPs) exhibit quantum size effects leading to unique optical, electronic and catalytic properties. GNPs are used increasingly in much electrochemical detection since they enhance the electrode conductivity and facilitate the electron transfer, thus improving the analytical sensitivity and selectivity [23,24]. GNPs can also find their wide applications in biosensor and medical diagnosis due to their excellent compatibility with biomolecules. The decoration of GNPs to CNTs creates a new nano-hybrid material with the integrated properties of the two components. This nano-hybrid material can offer new opportunities for the development of biosensors with high analytical performance. For example, Qin developed an amperometric biosensor for the determination of choline using gold nanoparticles-decorated multiwalled carbon nanotubes [25]. Haghighi fabricated a novel electrochemiluminescence glucose biosensor base on MWCNTs–nanoAu nano-hybrids [26]. Kooshki performed the determination of tryptophan at a MWCNTs–nanoAu modified glassy carbon electrode [27].

As far as we know, the reports on the detection of cholesterol based on the direct electrochemistry of ChOx are few in number. In the present work, gold nanoparticles-decorated multiwalled carbon nanotubes (GNPs-MWCNTs) were successfully synthesized based on the reduction of $HAuCl_4$ in the presence of MWCNTs and were characterized via transmission electron microscopy. The prepared nanocomposites were employed as a conducting matrix to immobilize cholesterol oxidase (ChOx) and promote direct electrochemistry of enzyme on the electrode surface. A third-generation cholesterol biosensor was developed, exhibiting an excellent analytical performance in terms of linear dynamic range, selectivity, reproducibility and stability.

2. Experimental

2.1. Materials

ChOx (EC 1.1.3.6, from *Streptomyces sp.*, ≥ 20 U mg^{-1} protein, Sigma), Cholesterol ($\geq 99.0\%$, Sigma), ascorbic acid (AA, $\geq 99.0\%$, Fluka) and uric acid (UA, Aldrich) were used as received. Multiwalled carbon nanotubes (MWCNTs, $\geq 95\%$, 20–30 nm in diameter) were purchased from Shenzhen Nanotech Port Co., Ltd. (Shenzhen, China). The buffer for the assay was 0.1 M phosphate buffered saline (PBS), prepared by mixing stock standard solutions of Na_2HPO_4 and KH_2PO_4. A stock solution of 10 mmol L^{-1} cholesterol was prepared by dissolving 0.0387 g cholesterol in a 10-mL flask containing 0.5 mL of Triton X-100 and 0.5 mL isopropanol in a bath at 60 °C and diluting with 0.1 mol L^{-1} PBS (pH 7.0). The solution was stored at 4 °C in dark and was stable for 2 weeks. Other chemicals were of analytical reagent grade, and all aqueous solutions were prepared in Milli-Q ultrapure water.

2.2. Apparatus

Electrochemical measurement experiments were performed with a CHI660C electrochemical workstation (CH Instruments, China) by using a three-electrode electrolytic cell. Glassy carbon electrode (GCE, 3 mm in diameter) acted as the working electrode. A KCl saturated calomel electrode served as the reference electrode. A platinum plate served as the counter electrode. The sizes of the nanoscale composites were characterized ex situ by a JEM-3010 high resolution transmission electron microscope (HRTEM, JEOL, Japan). The images of the modified electrode surface were obtained with a JSM-6700F field emission scanning electron microscope (FESEM, JEOL, Japan).

2.3. Preparation of GNPs-MWCNTs and immobilization of ChOx on GCE surface

The carboxyl group functionalized MWCNTs (MWCNTs–COOH) were synthesized by refluxing MWCNTs with nitric acid as described previously [28]. Briefly, MWCNTs with 70% nitric acid were sonicated for 20 min in a round bottom flask to get a homogeneous mixture and then refluxed for 18 h at 110 °C. The mixture was filtered under vacuum through a 0.22 μm millipore polycarbonate membrane and washed with distilled water until the pH of the filtrate became 7. The resulting MWCNTs–COOH was dried under vacuum for 30 h at 50 °C. Then, the 2 mg functionalized MWCNTs were suspended in 99 mL of $HAuCl_4$ solution by sonication for 10 min to make nanotubes dispersed equally. The aqueous solution was heated to boiling in a round-bottom flask. 1 mL trisodium citrate was added to this solution drop by drop under vigorous stirring for 20 min. The color of the solution changed from black to black red, indicating the formation of gold nanoparticles. After the heating was stopped, the mixed solution was stirred continuously until it was cooled to room temperature. The prepared GNPs-MWCNTs were separated by centrifugation (10,000 rpm) and re-suspended with 1 mL N,N-dimethylformamide (DMF). It was stored in a brown glass bottle at 4 °C for further use. As shown in Table 1, five composites were prepared and named as Nanocomposites 1, 2, 3, 4 and 5, respectively, based on the different contents of reactants in the mixed solution containing MWCNTs, $HAuCl_4$ and trisodium citrate for preparation of GNPs-MWCNTs.

Prior to modification, the GCE was polished with 0.05 μm α-Al_2O_3 power slurries until a mirror shiny surface appeared, and was sonicated sequentially in acetone, HNO_3 (1:1, v/v), NaOH (1 M) and ultrapure water for 3 min. 3 μL of GNPs-MWCNTs suspension was dropped on the GCE surface and allowed to dry at room temperature for 12 h. The ChOx/GNPs-MWCNTs/GCE surface was obtained by dropping 10 μL of the 100 U mL^{-1} ChOx solution on the modified electrode surface and it was dried in a refrigerator at 4 °C for 12 h. To maintain the stability of modified GCE, a drop of 5 μL 0.5% Nafion solution was cast on the membrane and allowed to dry in air for about 1 h. The electrode was gently washed with ultrapure water and then nitrogen-dried after every assembly process. The prepared Nafion/ChOx/GNPs-MWCNTs/GCE was stored at 4 °C when not in use.

2.4. Electrochemical measurement

All experiments were carried out at the ambient temperature of the laboratory in 0.1 mol L^{-1} PBS buffer as the supporting electrolyte. Cyclic voltammetry measurements were carried out in nitrogen-saturated solutions by bubbling pure nitrogen for 20 min and maintained under nitrogen atmosphere during measurements. The differential pulse voltammetry (DPV) measurements for cholesterol detection were performed from −0.2 to −0.7 V with a pulse amplitude of 25 mV and width of 50 ms in air-saturated solutions.

3. Results and discussion

3.1. Characterization of Nafion/ChOx/GNPs-MWCNTs/GCE

Fig. 1A shows the TEM image of the prepared GNPs-MWCNTs composites. The interlacing bundles of MWCNTs of about 30 nm in diameter can be found. Instead of smooth films, regularly shaped rounded gold nanoparticles were decorated on the nanotubes surface. The diameter of GNPs varies from 6 to 10 nm. Moreover, the nanoparticles were scarcely observed in the background, indicating the high selective nucleation of GNPs on the surface of functional MWCNTs. The images of GNPs-MWCNTs film, ChOx/GNPs-MWCNTs film and Nafion/ChOx/GNPs-MWCNTs on the GCE surface are shown in Fig. 1B–D. One can find that GNPs-MWCNTs were twisted together and a three dimensional homogeneous structure was obtained on GCE. This incompact structure could provide more effective active sites, which might play important roles in their electrochemical activities and biocompatibility for ChOx immobilization. When ChOx was adsorbed onto the GNPs-MWCNTs film, the enzyme covered the surface randomly with a clear unsaturated area. After the immobilization of Nafion, the electrode surface presented a porous membrane with a pore size of 200 nm. It is reported that the volume of a cholesterol molecules in the crystal structure is calculated to be 4.984 nm^3 [29]. So, cholesterol could easily penetrate through the Nafion membrane and arrive at the immobilized ChOx on the electrode surface.

Table 1
Prepared GNPs-MWCNTs nanocomposites.

Number of nanocomposites	The contents of reactants in the mixed solution for preparation of GNPs-MWCNTs (100 mL)			Amount of substance of GNPs on GNPs-MWCNTs loaded on GCE surface (pmol)[a]
	MWCNTs (mg mL^{-1})	$HAuCl_4$ (%)	Trisodium citrate (%)	
1	0.02	0.02	8	6.87 ± 0.34
2	0.02	0.04	16	7.73 ± 0.43
3	0.02	0.06	24	8.75 ± 0.19
4	0.02	0.08	32	12.0 ± 0.28
5	0.02	0.10	40	17.6 ± 0.35

[a] Results are presented as mean ± SD of triplicate experiments.

3.2. Direct electron transfer of ChOx on GNPs-MWCNTs film

Fig. 2 exhibits the cyclic voltammograms of GCE, MWCNTs/GCE, Nafion/ChOx/MWCNTs/GCE, GNPs-MWCNTs/GCE, and Nafion/ChOx/GNPs-MWCNTs/GCE in nitrogen-saturated pH 7.0 PBS. No redox peaks can be observed at GCE, MWCNTs/GCE and GNPs-MWCNTs/GCE in the potential ranges of −0.1 and 0.7 V in PBS (curves a, b and d), although the nanomaterial modified electrodes presented the bigger background currents. Nafion/ChOx/MWCNTs/GCE and Nafion/ChOx/GNPs-MWCNTs/GCE produced a pair of redox peaks at −0.39 V and −0.33 V, respectively (curves c and e). They should result from mutual conversion of the electroactive center, FAD/$FADH_2$, of the immobilized ChOx. Similar current peaks can be found on some modified electrodes by ChOx and nanomaterials [12–14].

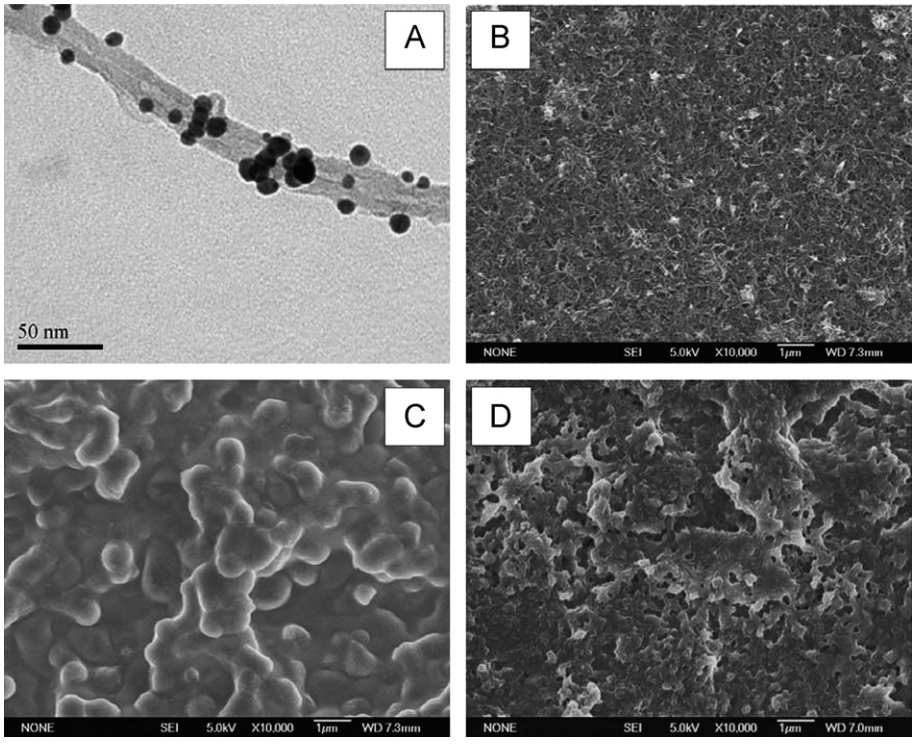

Fig. 1. (A) TEM image of GNPs-MWCNTs. (B–D) FESEM images of GNPs-MWCNTs/GCE, ChOx/GNPs-MWCNTs/GCE and Nafion/ChOx/GNPs-MWCNTs/GCE. Magnification: 10,000 ×.

One can notice that the currents of redox peaks in curve e were significantly higher than those in curve c. It indicates that GNPs-MWCNTs had more advantages than MWCNTs in facilitating the electron transfer between ChOx and the electrode surface. There were probably van der Waals forces, hydrogen bonding and π–π stacking interaction between enzyme and the activated MWCNTs containing lots of carboxyl groups. So, some ChOx molecules could be adsorbed on MWCNTs. The increased electrochemical signals of ChOx on GNPs-MWCNTs might be attributed to two factors. ChOx could be stably combined on GNPs-MWCNTs due to the S–Au bond between enzyme and GNPs besides the interaction between ChOx and MWCNTs. In addition, the larger exposed surface area of the nanotube composites after GNPs-decoration led to the higher enzyme-loading amount. Here, our experimental results prove that GNPs-MWCNTs linked ChOx to GCE and efficiently realized the direct electron transfer between them.

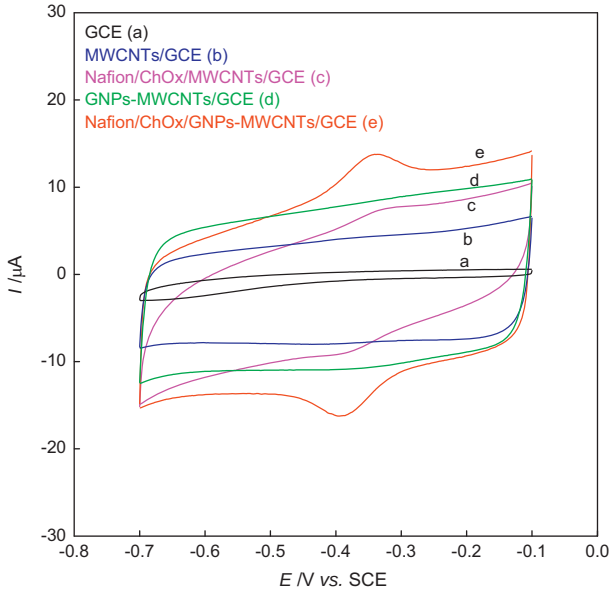

Fig. 2. Cyclic voltammograms of GCE (a), MWCNTs/GCE (b), Nafion/ChOx/MWCNTs/GCE (c), GNPs-MWCNTs/GCE (d) and Nafion/ChOx/GNPs-MWCNTs/GCE (e) in nitrogen-saturated 0.1 mol L^{-1} pH 7.0 PBS at 100 mV s^{-1}.

3.3. Optimization of Nafion/ChOx/GNPs-MWCNTs/GCE

It is concluded from Fig. 2 that GNPs could promote the immobilization of enzyme on the nanocomposites. In our opinion, the amount of gold on GNPs-MWCNTs should have some influence on the ChOx adsorption. The five kinds of GNPs-MWCNTs were obtained using the different $HAuCl_4$–trisodium citrate formula. Fig. S1 shows the cyclic voltammograms of the GNPs-MWCNTs modified GCE in the potential range of 0 and 1.3 V in pH 7.0 PBS. A pair of redox peaks (I and I′) (E_{pc}=0.5 V, E_{pa}=1.0 V) could be found, respectively. They should be derived from the mutual transformation between Au^0 and its oxidation production, Au_nO_m or $Au(OH)_x$, which was widely reported [30]. The amount of substance of Au^0 particles on the nanocomposite was calculated using the equation $n=Q/zF$, where Q is the charge used for the reduction of AuO to Au^0, F is the Faraday constant and z is the number of electrons transferred for the formation of Au^0 (Au(II) to Au^0, $z=2$), respectively. It can be found from Table 1 that the gold-amount was increased with the augment of $HAuCl_4$ and trisodium citrate contents. The effect of gold-loading on GNPs-MWCNTs on the amperometric response of Nafion/ChOx/GNPs-MWCNTs/GCE was revealed, and the results are shown in Fig. 3A. The background currents of cyclic voltammograms rose with the increase of gold-amount, suggesting growing GNPs loading. At the same time, the redox peak currents of the immobilized ChOx increased significantly and reached a maximum value at a gold-amount of 12.0 pmol. When the gold-amount exceeded this value, the redox peak currents began to decrease. The experimental results prove that immobilization of ChOx was closely related to gold loading. The specific surface area of GNPs-MWCNTs would be enhanced with the increase of GNPs on the nanocomposites. It undoubtedly benefited the ChOx adsorption. But too many products derived from the chemical reaction might enlarge the diameter of GNPs, even lead to gold-atom packing, which could reduced the specific surface area of GNPs. As a result, the adsorption of ChOx was weakened, accompanied with the decreased redox peak currents. In order to optimize the performance of the enzyme–nanocomposite modified electrode, in our work, no. 4 GNPs-MWCNT was used in preparation of Nafion/ChOx/GNPs-MWCNTs/GCE in all

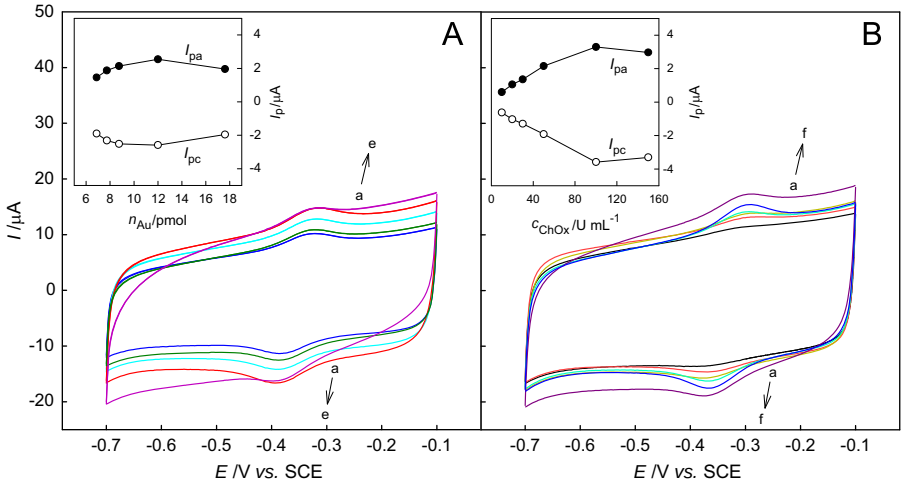

Fig. 3. (A) Cyclic voltammograms of Nafion/ChOx/GNPs-MWCNTs/GCE with different gold nanoparticle-loading in nitrogen-saturated 0.1 mol L^{-1} pH 7.0 PBS at 100 mV s^{-1}. The amount of substance of gold in GNPs-MWCNTs loaded on GCE surface: 6.87, 7.73, 8.75, 12.0 and 17.6 pmol (from a to e). The concentration of ChOx dropped on GNPs-MWCNTs/GCE: 100 U mL^{-1}. Insert: plot of the peak current (I_p) vs. the amount of substance of gold loaded on MWCNTs. (B) Cyclic voltammograms of Nafion/ChOx/GNPs-MWCNTs/GCE with different ChOx loading in nitrogen-saturated 0.1 mol L^{-1} pH 7.0 PBS at 100 mV s^{-1}. The concentration of ChOx dropped on GNPs-MWCNTs/GCE: 10, 20, 30, 50, 100 and 150 U mL^{-1} (from a to f). The amount of substance of GNPs loaded on MWCNTs: 12.0 pmol. Insert: plot of the peak current (I_p) vs. the concentration of ChOx.

subsequent experiments. The influence of ChOx loading on the amperometric response of Nafion/ChOx/GNPs-MWCNTs/GCE was also investigated. Fig. 3B shows that the redox peak currents of the modified GCE expressed an ascending trend, followed by some descending with the enhancement of the ChOx concentration. The decreased electrochemical signal displayed by 150 U mL^{-1} ChOx means that the immobilized enzyme film was too thick to effectively transfer electrons. Based on the above investigation, the concentration of ChOx at 100 U mL^{-1} was selected for the optimized condition.

3.4. Kinetics of ChOx on the modified electrode

Fig. 4A shows the cyclic voltammograms of the enzyme modified GCE in nitrogen-saturated 0.1 mol L^{-1} pH 7.0 PBS at scan rates. One can find that the redox peak current increased gradually with the rise of the scan rate accompanied by the positive shift of the anodic peak and the negative shift of the cathodic peak. Both the anodic and cathodic peak currents were linear with the scan rate in the range of 50–300 mV s^{-1}, being the characteristic of surface-controlled electrode process. A linear relationship between the peak current and the square root of scan rate was obtained at scan rates over 300 mV s^{-1}, demonstrating that the electrode reaction was a diffusion-controlled process at high scan rates. As we know, protons participate in the redox process of enzyme. The electrochemical reaction of ChOx immobilized on GNPs-MWCNTs at high scan rates could produce a proton gradient. The involvement of the proton gradient result in an electron transfer process with diffusion-controlled behavior [31]. The diffusion of protons from the solution to the electrode surface was the rate-limiting step at the scan rate more than 300 mV s^{-1}. According to the Laviron equation, $I_p = nFQv/4RT$ [32], where F is the Faraday constant, Q is the charge integrated from the reduction peak, v is the scan rate, R is the molar gas constant and T is the thermodynamic temperature, the number of electrons involved in the electrochemical process (n) was calculated to be 2.01. The surface coverage of ChOx on GNPs-MWCNTs (Γ^*) was obtained to be 2.04×10^{-10} mol cm^{-2} based on Faraday's law, $Q = nFA\Gamma^*$ [33], where A is the effective surface area of the working electrode. The results imply that two electrons were involved in the redox process of ChOx and the immobilization of ChOx on GNPs-MWCNTs was in a monolayer level [34]. Fig. 4B exhibits the relationship of the peak potential (E_p) with the logarithm of scan rate ($\ln v$). A charge transfer coefficient α of 0.44 was obtained according to the equation $E_p = K - (RT/\alpha nF)(\ln v)$. The peak-to-peak separation (ΔE_p) was 62 mV at the scan rate 100 mV s^{-1}. The electron transfer rate constant k_s of ChOx on GNPs-MWCNTs was estimated to be 1.55 s^{-1} using the Laviron formula $k_s = mnFv/RT$ when $n\Delta E_p < 200$ mV [32], where m is a parameter related to the peak-to-peak separation.

Cyclic voltammetric measurements using Nafion/ChOx/GNPs-MWCNTs/GCE in PBS solution at different pH values were taken and the results are shown in Fig. 5. Both the anodic and the cathodic peak potentials shifted negatively with the increase of pH from 4.0 to 8.0. It means that the H^+ exchange participated in the electrochemical reaction of ChOx. The maximum current response occurred at pH 7.0. So, pH 7.0 PBS was employed in the subsequent cholesterol detection. The relationship of the formal potential ($E^{0\prime} = (E_{pa} + E_{pc})/2$) with pH was shown in the inset of Fig. 6. The plots exhibited a linear relationship with a slope of -64 mV pH^{-1}, being close to the expected value of -59 mV pH^{-1}. It indicates that two protons participated in the electron transfer process.

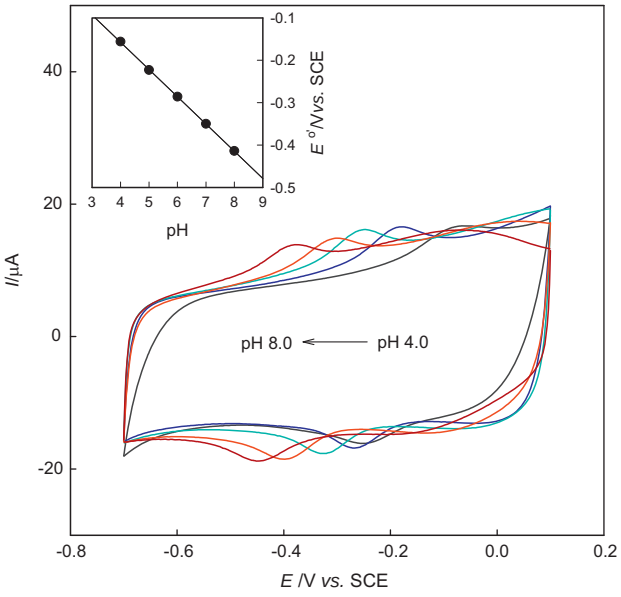

Fig. 5. Cyclic voltammograms of Nafion/ChOx/GNPs-MWCNTs/GCE in nitrogen-saturated 0.1 mol L^{-1} PBS with different pH values at 100 mV s^{-1}. Insert: $E^{0\prime}$ vs. pH.

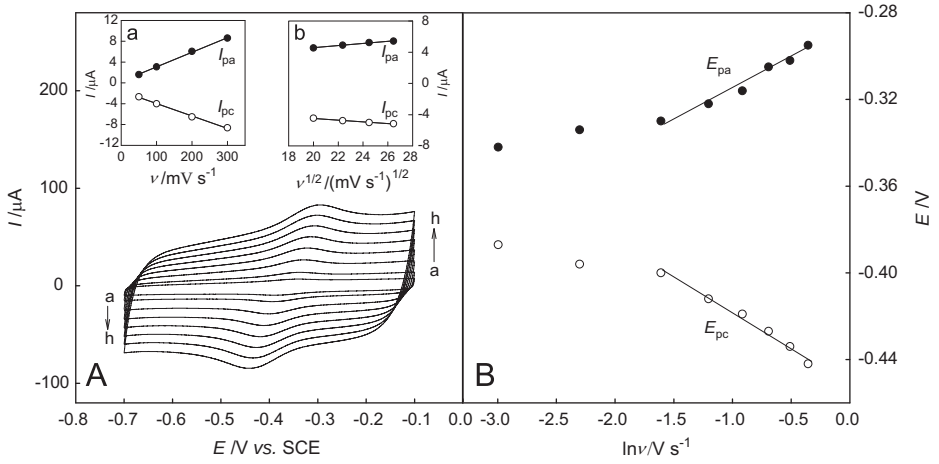

Fig. 4. (A) Cyclic voltammograms of Nafion/ChOx/GNPs-MWCNTs/GCE in nitrogen-saturated 0.1 mol L^{-1} pH 7.0 PBS at scan rates (v) of 50, 100, 200, 300, 400, 500, 600 and 700 mV s^{-1} (from a to h). Insert a: I_p vs. v. Insert b: I_p vs. $v^{1/2}$. (B) E_p vs. ln$v$.

3.5. Sensing application for cholesterol detection

Fig. 6 shows cyclic voltammograms of Nafion/ChOx/GNPs-MWCNTs/GCE in nitrogen- and air-saturated pH 7.0 PBS in the absence and presence of cholesterol. A pair of well-resolved redox peaks can be observed in nitrogen-saturated PBS. The cathodic peak current was larger and the anodic peak current was lower in the air-saturated solution as compared to the corresponding peaks in the nitrogen-saturated solution, indicating that dissolved oxygen participated in the redox process of the immobilized ChOx. In other words, the electrochemically formed ChOx ($FADH_2$) could electrocatalyze the reduction of dissolved oxygen according to the following equations.

$$\mathrm{ChOx(FAD)} + 2e^- + 2H^+ \rightleftharpoons \mathrm{ChOx(FADH_2)} \quad (1)$$

$$\mathrm{ChOx(FADH_2)} + O_2 \rightarrow \mathrm{ChOx(FAD)} + H_2O_2 \quad (2)$$

In addition, one can find an obvious cathodic peak at −0.53 V on the modified electrode in air-saturated PBS. It should be derived from the direct reduction of dissolved oxygen on the electrode surface.

When cholesterol was added into air-saturated PBS, the cathodic peak current decreased due to the enzymatic reaction between the oxidized form of ChOx (FAD) and cholesterol.

$$\mathrm{ChOx(FAD)} + \mathrm{cholesterol} \rightarrow \mathrm{ChOx(FADH_2)} + \mathrm{cholest{-}4{-}en{-}3{-}one} \quad (3)$$

The response of Nafion/ChOx/GNPs-MWCNTs/GCE to cholesterol reported in this work was employed for cholesterol detection. Fig. 7A shows the differential pulse voltammetry measurements using the ChOx modified electrode in air-saturated pH 7.0 PBS containing cholesterol with increasing concentration. The peak current decreased with negative shifts of peak potentials when the cholesterol content was enhanced. Fig. 7B exhibits plot of the peak current change (ΔI_p) before and after cholesterol introduction against the cholesterol concentration ($c_{cholesterol}$). Obviously, the ΔI_p value rose with deflexibility when the $c_{cholesterol}$ value increased. It can be found that these data were fitted well to the Langmuir adsorption model. As shown in the insert of Fig. 7B, $c_{cholesterol}/\Delta I_p$ exhibited a linear response with respect to $c_{cholesterol}$ over the range of cholesterol concentration from 0.0100 to 5.00 mmol L^{-1}. The regression equations was $c_{cholesterol}/\Delta I_p = 0.148 c_{cholesterol} + 0.0429$ with a high correlation coefficient of 0.997 and the detection limit was 4.3 μmol L^{-1} (based on S/N=3). The apparent Michalis–Menten constant (K_m), which indicates the enzyme–substrate kinetics, can be used to evaluate the biological activity of the immobilized enzyme. According to the Lineweaver–Burke equation, $1/v = 1/V_{max} + K_m/(V_{max}[S])$ [35], the corresponding plot yielded an apparent K_m value of 0.29 mmol L^{-1}, indicating ChOx immobilized on GNPs-MWCNTs had high affinity to cholesterol.

Table 2 gives the comparison of analytical parameters of some cholesterol biosensors using carbon nanotubes. Nafion/ChOx/GNPs-MWCNTs/GCE presents a broader linear range and acceptable detection limit compared with the other CNT-modified electrodes.

The interferences of some species which coexist with cholesterol in human serum were considered. Fig. S2 shows the peak current change caused by 0.1 mmol L^{-1} uric acid, 0.1 mmol L^{-1} ascorbic acid and 1.0 mmol L^{-1} glucose accounted for 2.49%, 7.72% and 2.94% of that derived from 1.0 mmol L^{-1} cholesterol, respectively, in an air-saturated pH 7.0 PBS solution. It proves that the developed biosensor had an acceptable selectivity.

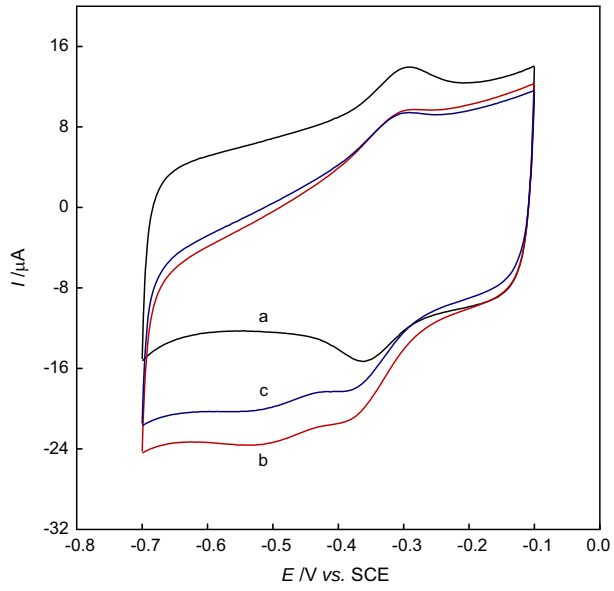

Fig. 6. Cyclic voltammograms of the Nafion/ChOx/GNPs-MWCNTs/GCE in nitrogen- (a) and air-saturated 0.1 mol L^{-1} pH 7.0 PBS before (b) and after (c) addition of 1.0 mmol L^{-1} cholesterol at 100 mV s^{-1}.

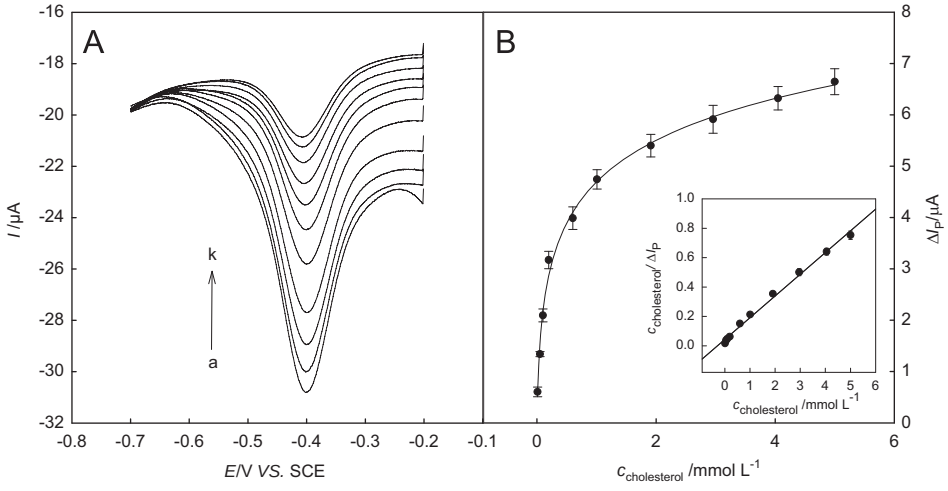

Fig. 7. (A) Differential pulse voltammograms of Nafion/ChOx/GNPs-MWCNTs/GCE in air-saturated 0.1 mol L^{-1} pH 7.0 PBS containing 0, 0.0100, 0.0498, 0.0990, 0.196, 0.602, 1.01, 1.91, 2.96, 4.05, and 5.00 mmol L^{-1} cholesterol (from a to k). (B) ΔI_p vs. $c_{cholesterol}$. Insert: $c_{cholesterol}/\Delta I_p$ vs. $c_{cholesterol}$. Results are presented as mean ± SD (error bar) of triplicate experiments.

Table 2
Comparison of analytical performance of some electrochemical cholesterol biosensors using carbon nanotubes.

Electrode	Linear range (mM)	Detection limit (μM)	Electrochemically measured species	References
MWCNTs–ChOx–SiO_2–CS/PB/GCE	0.004–0.7	1	PB	[36]
ChOx–MWNTs/SPCE	2.59–10.3 (100–400 mg dL^{-1})	–	$[Fe(CN)_6]^{3-}$	[37]
ChOx/sol–gel/Pt–CNTs/GRE	0.004–0.1	1.4	H_2O_2	[38]
ChOx/IL–CS/Au–(SH)MWNTs/ITO	0.5–5	–	H_2O_2	[39]
ChEt–ChOx/MWCNTs/SiO_2–CS/ITO	0.259–12.9 (10–500 mg dL^{-1})	16 (0.634 mg dL^{-1})	$[Fe(CN)_6]^{3-}$	[40]
ChOx/MWCNTs/GCE	0.0468–0.279	46.8	H_2O_2	[41]
ChOx/KMWNTs/GCE	0.00005–0.016	0.005	ChOx	[12]
(PDDA–[MWCNTs–$ChOx]_5$)/GRE	0.1–1.0	30	ChOx	[13]
Nafion/ChOx/GNPs-MWCNTs/GCE	0.01–5.0	4.3	ChOx	This work

CS: chitosan, PB: Prussian blue, SPCE: screen-printing carbon electrode, GRE: graphite electrode, IL: ionic liquid, ITO: indium tin oxide coated glass, ChEt: cholesterol esterase, KMWNTs: potassium-doped multi-walled carbon nanotubes, PDDA: poly(diallyldimethylammonium chloride).

The repeatability of the biosensor was investigated. Surely it is not easy to confirm that the prepared GNPs-MWCNTs materials in different batches were identical because such special conditions as stirring and heating were involved in the preparation-progress of nanocomposites. But the prepared GNPs-MWCNTs in same batch owned the satisfactory uniformity and could maintain excellent stability in a long time. The relative standard deviation (RSD) of current responses for 1 mM cholesterol in air-saturated PBS at three electrodes, which were independently prepared with the synthesized GNPs-MWCNTs composites in same batch and the same amount of ChOx and Nafion, was 5.8%, revealing an acceptable repeatability in the construction of the biosensor. The reproducibility of the cholesterol biosensor was investigated by detecting 1 mmol L^{-1} cholesterol successively in air-saturated PBS for five times using the same modified electrode. The relative standard deviation (RSD) was 4.8%, demonstrating that the biosensor has a good reproducibility. Additional experiments were carried out to test the stability. The enzyme-modified electrode was stored at 4 °C when it was not in use. It could keep 95% of its initial current response to cholesterol within 2 weeks, indicating that the GNPs-MWCNTs composite and Nafion were very efficient for retaining the activity of ChOx.

The analysis of free cholesterol in serum was performed using the developed biosensor without sample pretreatment. The cholesterol concentration in a serum sample was determined to be 1.86 mmol L^{-1}. This value agreed with that from a routine spectrophotometric method (using cholesterol oxidase and peroxidase), 1.76 mmol L^{-1}, with a relative error of 4%. The recovery tests were conducted by adding 0.4 mmol L^{-1}, 0.6 mmol L^{-1} and 1.0 mmol L^{-1} cholesterol to the serum sample, which produced the recovery of $96.3 \pm 2.3\%$, $104 \pm 3.7\%$ and $105 \pm 5.5\%$, respectively, demonstrating a good accuracy for the determination of cholesterol in real samples.

4. Conclusions

GNPs-MWCNTs composites were fabricated using multiwalled carbon nanotubes based on the reduction reaction of $HAuCl_4$ in solution. ChOx was dropped on the nanocomposite modified GCE surface and was protected by a Nafion film. Gold nanoparticles decorated on MWCNTs could immobilize the enzyme due to van der Waals force, hydrogen bonding and the Au–S bond, effectively promoting the direct electron transfer between the enzyme molecules and the electrode. The direct electrochemistry of ChOx was a two proton participated two-electron redox process. The developed biosensor exhibited favorable electrocatalytic property to cholesterol, with a linear range from 0.0100 to 5.00 mmol L^{-1} and a detection limit of 4.3 μmol L^{-1} (S/N=3). In addition, the sensor presented good selectivity, repeatability, reproducibility, stability and accuracy for real sample measurement. All these characteristics suggest that this work presents a good platform for the electrochemical detection of cholesterol using the third-generation enzyme biosensor.

Acknowledgments

This work was supported by the National Natural Science Foundation of China (Grant no. 20905025), Hunan Provincial Natural Science Foundation of China (Grant no. 12JJ3015), the Program for Excellent Talents in Hunan Normal University (Grant no. ET12203) and Aid program for Science and Technology Innovative Research Team in Higher Educational Institutions of Hunan Province.

Appendix A. Supporting information

Supplementary data associated with this article can be found in the online version at http://dx.doi.org/10.1016/j.talanta.2012.12.036.

References

[1] R. Bittman, Cholesterol: Its Functions and Metabolism in Biology and Medicine, Plenum, New York, 1997.
[2] M. Sungano, A.C. Beynen, Dietary Proteins, Cholesterol Metabolism and Atherosclerosis, S Karger AG, Basel, 1990.
[3] A.P. Kenny, Biochem. J. 52 (1952) 611–619.
[4] E. Agulló, B.S. Gelós, Food Res. Int. 29 (1996) 77–80.
[5] W.W. Wong, D.L. Hachey, L.L. Clarke, S. Zhang, M. Llaurador, W.G. Pond, Appl. Radiat. Isot. 45 (1994) 529–533.
[6] Ö. Türkarslan, S.K. Kayahan, L. Toppare, Sens. Actuators B 136 (2009) 484–488.
[7] M. Ahmad, C. Pan, L. Gan, Z. Nawaz, J. Zhu, Highly Sensitive. J. Phys. Chem. C 114 (2010) 243–250.
[8] U. Saxena, M. Chakraborty, P. Goswami, Biosens. Bioelectron. 26 (2011) 3037–3043.
[9] R.M. Iannlello, A.M. Yacynych, Anal. Chem. 53 (1981) 2090–2095.
[10] T. Nakaminami, S. Ito, S. Kuwabata, H. Yoneyama, Anal. Chem. 71 (1999) 1068–1076.
[11] B.D. Malhotra, A. Kaushik, Thin Solid Films 518 (2009) 614–620.
[12] X. Li, J. Xu, H. Chen, Electrochim. Acta 56 (2011) 9378–9385.
[13] R. Manjunatha, D.H. Nagaraju, G.S. Suresh, J.S. Melo, S.F. D'souza, T.V. Venkatesha, J. Electroanal. Chem. 651 (2011) 24–29.
[14] R. Manjunatha, G.S. Suresh, J.S. Melo, S.F. D'Souza, T.V. Venkatesha, Talanta 99 (2012) 302–309.
[15] G.A. Rivas, M.D. Rubianes, M.C. Rodríguez, N.F. Ferreyra, G.L. Luque, M.L. Pedano, S.A. Miscoria, C. Parrado, Talanta 74 (2007) 291–307.
[16] Y. Yin, P. Wu, Y. Lü, P. Du, Y. Shi, C. Cai, J. Solid State Electrochem. 11 (2007) 390–397.
[17] L. Wang, L. Wei, Y. Chen, R. Jiang, J. Biotechnol. 150 (2010) 57–63.
[18] S. Alwarappan, G. Liu, C.Z. Li, Nanomed. Nanotechnol. 6 (2010) 52–57.
[19] J. Zhang, M. Feng, H. Tachikawa, Biosens. Bioelectron. 22 (2007) 3036–3041.
[20] H. Zhang, Z. Meng, Q. Wang, J. Zheng, Sens. Actuators B 158 (2011) 23–27.

[21] Y. Zhao, W. Zhang, H. Chen, Q. Luo, S.F.Y. Li, Sens. Actuators B 87 (2002) 168–172.
[22] Z. Wang, M. Li, P. Su, Y. Zhang, Y. Shen, D. Han, A. Ivaska, L. Niu, Electrochem. Commun. 10 (2008) 306–310.
[23] R.N. Goyal, V.K. Gupta, M. Oyama, N. Bachheti, Electrochem. Commun. 7 (2005) 803–807.
[24] R.N. Goyal, V.K. Gupta, M. Oyama, N. Bachheti, Electrochem. Commun. 8 (2006) 65–70.
[25] X. Qin, H. Wang, X. Wang, Z. Miao, L. Chen, W. Zhao, M. Shan, Q. Chen, Sens. Actuators B 147 (2010) 593–598.
[26] B. Haghighi, S. Bozorgzadeh, L. Gorton, Sens. Actuators B 155 (2011) 577–583.
[27] M. Kooshki, H. Abdollahi, S. Bozorgzadeh, B. Haghighi, Electrochim. Acta 56 (2011) 8618–8624.
[28] S. Aryal, K.C.R. Bahadur, N. Dharmaraj, K.W. Kim, H.K. Kim, Scr. Mater. 54 (2006) 131–135.
[29] C. Hofsäβ, E. Lindahl, O. Edholm, Biophys. J. 84 (2003) 2192–2206.
[30] G. Tremiliosi-Filho, L.H. Dall'Antonia, G. Jerkiewicz, J. Electroanal. Chem. 422 (1997) 149–159.
[31] A.P. Brown, F.C. Anson, J. Electroanal. Chem. 92 (1978) 133–145.
[32] E. Laviron, J. Electroanal. Chem. 101 (1979) 19–28.
[33] J. Wang, Analytical Electrochemistry, third ed., Wiley-VCH, Hoboken, 2006.
[34] Y. Liu, L. Liu, S. Dong, Electroanal. 19 (2007) 55–59.
[35] D.L. Scott, E.F. Bowden, Anal. Chem. 66 (1994) 1217–1223.
[36] X. Tan, M. Li, P. Cai, L. Luo, X. Zou, Anal. Biochem. 337 (2005) 111–120.
[37] G. Li, J.M. Liao, G.Q. Hu, N.Z. Ma, P.J. Wu, Biosens. Bioelectron. 20 (2005) 2140–2144.
[38] Q. Shi, T. Peng, Y. Zhu, C.F. Yang, Electroanal. 17 (2005) 857–861.
[39] A.L. Gopalan, K.P. Lee, D. Ragupathy, Biosens. Bioelectron. 24 (2009) 2211–2217.
[40] P.R. Solanki, A. Kaushik, A.A. Ansari, A. Tiwari, B.D. Malhotra, Sens. Actuators B 137 (2009) 727–735.
[41] J.Y. Yang, Y. Li, S.M. Chen, mat Lin, Int. J. Electrochem. Sci. 6 (2011) 2223–2234.